



5-19-2009

A wide-band-gap p-type thermoelectric material based on quaternary chalcogenides of $\text{Cu}_2\text{ZnSnQ}_4$ (Q=S,Se)

Min-Ling Liu
Chinese Academy of Sciences

Fu-Qiang Huang
Chinese Academy of Sciences

Li-Dong Chen
Chinese Academy of Sciences

I-Wei Chen
University of Pennsylvania, iweichen@seas.upenn.edu

Follow this and additional works at: http://repository.upenn.edu/mse_papers

Recommended Citation

Liu, M., Huang, F., Chen, L., & Chen, I. (2009). A wide-band-gap p-type thermoelectric material based on quaternary chalcogenides of $\text{Cu}_2\text{ZnSnQ}_4$ (Q=S,Se). Retrieved from http://repository.upenn.edu/mse_papers/170

Copyright 2009 American Institute of Physics. This article may be downloaded for personal use only. Any other use requires prior permission of the author and the American Institute of Physics. Reprinted from:

A wide-band-gap p-type thermoelectric material based on quaternary chalcogenides of $\text{Cu}_2\text{ZnSnQ}_4$ (Q= S,Se) Min-Ling Liu, Fu-Qiang Huang, Li-Dong Chen, and I-Wei Chen, *Appl. Phys. Lett.* 94, 202103 (2009), DOI:10.1063/1.3130718

Publisher URL: <http://link.aip.org/link/?APPLAB/94/202103/1>

This paper is posted at ScholarlyCommons. http://repository.upenn.edu/mse_papers/170

For more information, please contact libraryrepository@pobox.upenn.edu.

A wide-band-gap p-type thermoelectric material based on quaternary chalcogenides of $\text{Cu}_2\text{ZnSnQ}_4$ (Q=S,Se)

Abstract

Chalcopyritelike quaternary chalcogenides, $\text{Cu}_2\text{ZnSnQ}_4$ (Q=S,Se), were investigated as an alternative class of wide-band-gap p-type thermoelectric materials. Their distorted diamondlike structure and quaternary compositions are beneficial to lowering lattice thermal conductivities. Meanwhile, partial substitution of Cu for Zn creates more charge carriers and conducting pathways via the CuQ_4 network, enhancing electrical conductivity. The power factor and the figure of merit (ZT) increase with the temperature, making these materials suitable for high temperature applications. For $\text{Cu}_{2.1}\text{Zn}_{0.9}\text{SnQ}_4$, ZT reaches about 0.4 at 700 K, rising to 0.9 at 860 K.

Keywords

ELECTRONIC-STRUCTURE, THIN-FILMS, SN, SEMICONDUCTOR, TRANSPORT, CRYSTAL, SYSTEM

Comments

Copyright 2009 American Institute of Physics. This article may be downloaded for personal use only. Any other use requires prior permission of the author and the American Institute of Physics. Reprinted from:

A wide-band-gap p-type thermoelectric material based on quaternary chalcogenides of $\text{Cu}_2\text{ZnSnQ}_4$ (Q = S,Se) Min-Ling Liu, Fu-Qiang Huang, Li-Dong Chen, and I-Wei Chen, *Appl. Phys. Lett.* 94, 202103 (2009), DOI:10.1063/1.3130718

Publisher URL: <http://link.aip.org/link/?APPLAB/94/202103/1>

A wide-band-gap *p*-type thermoelectric material based on quaternary chalcogenides of $\text{Cu}_2\text{ZnSnQ}_4$ ($Q=\text{S}, \text{Se}$)

Min-Ling Liu,¹ Fu-Qiang Huang,^{1,a)} Li-Dong Chen,¹ and I-Wei Chen²

¹CAS Key Laboratory of Materials for Energy Conversion, Shanghai Institute of Ceramics, Chinese Academy of Sciences, 1295 Dingxi Road, Shanghai 200050, People's Republic of China

²Department of Materials Science and Engineering, University of Pennsylvania, Philadelphia, Pennsylvania 19104-6272, USA

(Received 14 January 2009; accepted 13 April 2009; published online 19 May 2009)

Chalcopyritelike quaternary chalcogenides, $\text{Cu}_2\text{ZnSnQ}_4$ ($Q=\text{S}, \text{Se}$), were investigated as an alternative class of wide-band-gap *p*-type thermoelectric materials. Their distorted diamondlike structure and quaternary compositions are beneficial to lowering lattice thermal conductivities. Meanwhile, partial substitution of Cu for Zn creates more charge carriers and conducting pathways via the CuQ_4 network, enhancing electrical conductivity. The power factor and the figure of merit (*ZT*) increase with the temperature, making these materials suitable for high temperature applications. For $\text{Cu}_{2.1}\text{Zn}_{0.9}\text{SnQ}_4$, *ZT* reaches about 0.4 at 700 K, rising to 0.9 at 860 K. © 2009 American Institute of Physics. [DOI: 10.1063/1.3130718]

Thermoelectric (TE) materials can convert thermal energy to electrical energy (Seebeck effect) or vice versa (Peltier effect). The figure of merit of TE materials is a dimensionless quantity, $ZT=(S^2\sigma/\kappa)T$, where *T* is the absolute temperature, *S* is the Seebeck coefficient, and σ and κ are the electrical and thermal conductivity, respectively. Several binary chalcogenides are known to have high *ZT* (Refs. 1–7) (a summary is given in Table S1 of supporting information⁸). Within this group, a large band gap E_g is correlated with a low σ , a high *S*, and a low κ , and vice versa. In general, it is difficult to achieve a high *S*, high σ , and low κ in the same material, especially in a *p*-type semiconductor with a large E_g .

There is a similar challenge in the *p*-type transparent conductive material in that a large E_g is usually correlated with a high transmittance (of visible light) but low σ , and vice versa. Recently, we proposed to meet this challenge by constructing materials with two structural/functional units, one electrically conducting and the other insulating, one example being Cu-doped chalcopyrite-type CuAlS_2 that has a wide band gap (about 3.4 eV) and a high σ .^{9–12} Note that chalcopyrites, having a diamondlike tetrahedral framework structure, already include some low-phonon-conductive materials, such as Cu_2SnS_3 and Cu_2SnSe_3 ,^{13–17} which are used for infrared transmission. Therefore, it would be interesting to investigate whether the low phonon conduction can survive σ -enhancing doping in these large band-gap *p*-type semiconductors, thereby providing alternative TE materials.

Specifically, following the concept of two structural/functional units, we propose a doping strategy that enhances σ by providing more holes in the electrically conducting pathway, and suppresses κ by disordering the insulating pathway. Toward the latter end, a quaternary compound should be advantageous over a ternary one, so the series of $\text{Cu}_2\text{ZnSnQ}_4$ ($Q=\text{S}, \text{Se}$) is chosen for exploratory studies. These materials are already known as potential (In-free) photovoltaic materials due to their appropriate E_g (1.4–1.5

eV).^{18–20} Structurally, $\text{Cu}_2\text{ZnSnS}_4$ and $\text{Cu}_2\text{ZnSnSe}_4$ crystallize in the kesterite and stannite structure types [Fig. 1(a)], respectively.²¹ The two structural units are (a) the $[\text{Cu}_2\text{Q}_4]$ tetrahedral slabs, which may be viewed as conducting, and (b) the $[\text{SnZnQ}_4]$ tetrahedral slabs, which may be viewed as insulating. In analogy to Cu doping of the Al site in *p*-type CuAlS_2 , it also follows that Cu doping of the Zn site could be an efficacious strategy to enhance σ on the $[\text{Cu}_2\text{Q}_4]$ network and, perhaps, to suppress κ by disordering the $[\text{SnZnQ}_4]$ slabs. To verify this strategy and to explore their potential for high temperature TE applications, we have studied their physical properties up to 860 K.

Powders of $\text{Cu}_2\text{ZnSnQ}_4$ and $\text{Cu}_{2.1}\text{Zn}_{0.9}\text{SnQ}_4$ ($Q=\text{S}, \text{Se}$) were synthesized by solid state reaction of stoichiometric amounts of Cu (99.999%, SinoReag), Zn (99.99%, SinoReag), Sn (99.999%, SinoReag), and S/Se (99.999%, SinoReag) powders in a sealed fused silica tube evacuated to ≤ 1 Pa argon. The samples were slowly heated to 923 K at

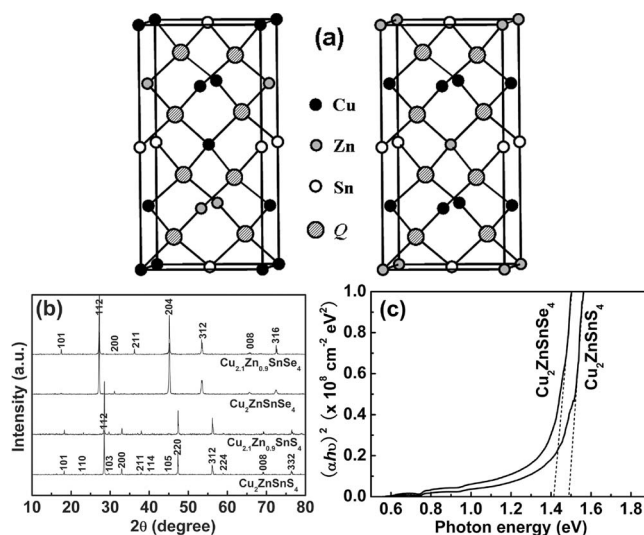


FIG. 1. Crystal structure (a) of kesterite (left) for $Q=\text{S}$ and stannite (right) for $Q=\text{Se}$, powder XRD patterns (b) and absorption spectra (c) of $\text{Cu}_2\text{ZnSnQ}_4$ and $\text{Cu}_{2.1}\text{Zn}_{0.9}\text{SnQ}_4$ ($Q=\text{S}, \text{Se}$).

^{a)}Author to whom correspondence should be addressed. Electronic mail: huangfq@mail.sic.ac.cn.

0.5 and 2 K/min for sulfides and selenides, respectively, held for 48 h, and furnace cooled to the room temperature. The harvested powders were grounded, sealed, and calcined for 96 h at 1123 and 1073 K for sulfides and selenides, respectively. The final powders were consolidated in a spark plasma sintering furnace in a graphite die ($\Phi 10$ mm) under a pressure of 60 MPa at 1073 K (for sulfides) and 1023 K (for selenides), held for 5 min in an argon atmosphere. The measured relative densities of all the samples were about 97%.

X-ray diffraction (XRD) patterns of the bulk samples were obtained (Rigaku D/Max-2550 V) using Cu $K\alpha$ radiation ($\lambda=0.154$ 18 nm) and their compositional homogeneity was examined by electron probe microanalysis (EPMA) (JEOL, JXA-8100). Optical absorption spectra of their pulverized powders were measured at room temperature by a UV-visible-near IR spectrometer (HITACHI U-3010) equipped with an integrating sphere. For transport property measurements, bar samples about $1.5 \times 2 \times 10$ mm³ were used. Electrical conductivity was measured by a four-probe method. Thermoelectromotive force (ΔE) at the test temperature was measured using five different temperature gradients ($0 \text{ K} < \Delta T < 2 \text{ K}$) to calculate the Seebeck coefficient from the ΔE versus ΔT plot. Thermal diffusivity coefficient λ was determined using a laser flash method in a flowing Ar atmosphere (Netzsch LFA 427). The thermal conductivity was calculated from $\kappa = \rho \lambda C_p$, where ρ is the density and C_p is the specific heat capacity. The above physical properties were measured up to 700 K. Hall coefficients were measured in an Accent HL5500 Hall System at room temperature. Additional experiments at 860 K were also performed for one material as will be described later.

The XRD patterns [Fig. 1(b)] and EPMA (not shown) verified that the samples are phase pure and homogeneous, as all the diffractions peaks can be indexed as $\text{Cu}_2\text{ZnSnS}_4$ and $\text{Cu}_2\text{ZnSnSe}_4$.²⁰ After Cu doping, the lattice parameters of a and c decrease (evidenced by a slight peak shift toward higher angle and a small increase of peak splitting, data not shown), which may be attributed to the smaller Cu^{2+} compared to Zn^{2+} , and the more flattened tetrahedron of $\text{Cu}^{2+}Q_4$ compared to $\text{Zn}^{2+}Q_4$. At room temperature the optical data [Fig. 1(c)] plotted as $(\alpha h\nu)^2$ against photon energy, where α is absorption coefficient, h is the Planck constant, and ν is the wave number, give an estimated E_g of about 1.49 and 1.41 eV for $\text{Cu}_2\text{ZnSnS}_4$ and $\text{Cu}_2\text{ZnSnSe}_4$, respectively. These values are consistent with the reported data^{18–20} and much larger than those of typical binary TE materials.^{1–7} As expected, sulfide has a larger E_g than selenide due to more hybridization of Se $4p$ and Cu $3d$ at the valence band maximum (VBM).

The temperature spectra of σ for $\text{Cu}_2\text{ZnSnQ}_4$ and $\text{Cu}_{2.1}\text{Zn}_{0.9}\text{SnQ}_4$ ($Q=\text{S, Se}$) in Fig. 2(a) show a large increase from sulfide to selenide. For both, Cu doping results in a dramatic increase of σ reaching 2600 S m^{-1} for $\text{Cu}_{2.1}\text{Zn}_{0.9}\text{SnS}_4$ and 86 000 S m^{-1} for $\text{Cu}_{2.1}\text{Zn}_{0.9}\text{SnSe}_4$, which may be attributed to creation of holes [$\text{Cu}^{2+} 3d^9$ versus $\text{Cu}^+ 3d^{10}$] and conversion of insulating paths ($[\text{ZnQ}_4]$) to conducting paths ($[\text{CuQ}_4]$). Although $\text{Cu}_2\text{ZnSnS}_4$ is a normal semiconductor exhibiting a thermally activated behavior for σ , the strong thermal activation is largely removed by Cu doping. Selenide samples show a metallic behavior in analogy to the reported trend for LaCuOQ ($Q=\text{S, Se, Te}$): the sulfide and selenide are semiconducting and the telluride is

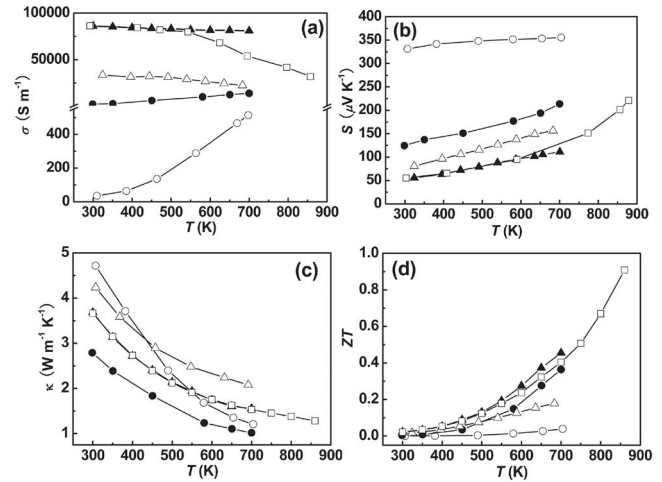


FIG. 2. Temperature dependence of electrical conductivity (a), Seebeck coefficient (b), total thermal conductivity (c) and figure of merit ZT (d) for $\text{Cu}_2\text{ZnSnS}_4$ (\circ), $\text{Cu}_{2.1}\text{Zn}_{0.9}\text{SnS}_4$ (\bullet), $\text{Cu}_{2.1}\text{Zn}_{0.9}\text{SnSe}_4$ (Δ), $\text{Cu}_{2.1}\text{Zn}_{0.9}\text{SnSe}_4$ (\blacktriangle), and sodium silicate coated $\text{Cu}_{2.1}\text{Zn}_{0.9}\text{SnSe}_4$ (\square) during first heating cycle. Note in (c) the symbols \blacktriangle and \square nearly coincide from 300 to 700 K.

metallic.²³ A flat $\sigma(T)$ has also been observed in LnCuOTe ($\text{Ln}=\text{La, Ce, Nd}$)²³ and is indicative of the metallic behavior with a relatively short mean free path limited by defect/impurity scattering rather than phonon scattering. These features are all consistent with the interpretation that hole conductivity comes from the hybridization of Cu $3d$ with $Q np$ ($Q np=\text{S } 3p, \text{ Se } 4p, \text{ Te } 5p$) near the VBM.²³

Hole conduction was verified by both positive Seebeck coefficients [Fig. 2(b)] and Hall coefficients for all the samples (Hall coefficients are listed in Table S2 of supporting information⁸). The Seebeck coefficients slightly increase with the temperature. These values are comparable to those of the well-known binary TE materials. Notably, both S and σ increase with the temperature in $\text{Cu}_2\text{ZnSnS}_4$, which was confirmed using duplicate samples and different measuring instruments (data not shown). The enhanced σ in doped $\text{Cu}_{2.1}\text{Zn}_{0.9}\text{SnQ}_4$ and the mostly positive temperature dependence of S and σ cause the power factors ($\text{PF}=S^2\sigma$) to increase especially at higher temperatures, reaching 0.58 and 1.01 $\text{mW m}^{-1} \text{K}^{-2}$ at 700 K for $\text{Cu}_{2.1}\text{Zn}_{0.9}\text{SnS}_4$ and $\text{Cu}_{2.1}\text{Zn}_{0.9}\text{SnSe}_4$, respectively (the PF plots are given in Figure S1 in supporting information⁸).

The κ values in Fig. 2(c) are all very low comparable to the binary TE materials.^{1–7} Their rapid decrease with the temperature indicates phonon conductivity is predominant. Interestingly, Cu doping lowers κ , suggesting a beneficial effect of disrupting the $[\text{Zn/SnQ}_4]$ tetrahedral slabs and distorting the diamondlike structure according to the XRD analysis. The lattice thermal conductivity (κ_L) may be estimated by subtracting the carrier thermal conductivity κ_E from κ , where the Wiedemann–Franz relation with a Lorenz constant of $L_0=2.0 \times 10^{-8} \text{ V}^2 \text{K}^{-2}$ is applied for estimating κ_E ($\kappa_E=L_0\sigma T$). Since the doped samples have a larger κ_E , after subtracting κ_E the remainder (i.e., κ_L) should reveal an even stronger suppression due to doping (the κ_L plots are given in Figure S2 in supporting information⁸). Therefore, the strategy of doping a two-structural/functional-unit material proves to be highly effective for both electrical and thermal conductivity in the quaternary compounds. Lastly, an increasing PF and a decreasing κ especially at higher tem-

peratures cause the dimensionless figure of merit ZT [Fig. 2(d)] to increase with Cu doping, with ZT at 700 K (the highest measuring temperature) reaching 0.36 and 0.45 for $\text{Cu}_{2.1}\text{Zn}_{0.9}\text{SnS}_4$ and $\text{Cu}_{2.1}\text{Zn}_{0.9}\text{SnSe}_4$, respectively.

The use of $\text{Cu}_2\text{ZnSnSe}_4$ is ultimately limited by a phase transition at about 883 K.¹⁸ In view of the rising trend of ZT with temperature, we have attempted measurements up to around 860 K using $\text{Cu}_{2.1}\text{Zn}_{0.9}\text{SnSe}_4$ bars side coated with a protective glass (sodium silicate) to prevent oxidation, sublimation, or decomposition. After several coats followed by drying, an overall coating thickness about 1.5 mm was achieved. For thermal conductivity measurements, the disk-shaped samples were also coated with graphite, which again slowed the sublimation process somewhat to allow reproducible data to be obtained. The data of coated $\text{Cu}_{2.1}\text{Zn}_{0.9}\text{SnSe}_4$ samples are plotted in Fig. 2 as open squares to compare with those of uncoated samples (filled triangles). The two sets of data are in agreement at low temperatures; above 500 K, the coated sample has a lower σ and a higher S . Such difference could be caused by a compositional change due to glass infiltration, and the change apparently occurred only during the first heating cycle since the data from the subsequent cooling and heating cycles are almost indistinguishable (the “hysteresis” plots are shown in Figure S3 of supporting information⁸). The data of coated samples give the following values at 860 K: $\sigma=31856 \text{ S m}^{-1}$, $S=206.7 \mu\text{V K}^{-1}$, and $\kappa=1.282 \text{ W m}^{-1} \text{ K}^{-1}$, resulting in a PF value of $1.35 \text{ mW m}^{-1} \text{ K}^{-2}$ and a ZT of 0.91. Since the errors of underestimating σ and overestimating S are mutually compensating to some extent, the value of ZT at 860 K is probably accurate, which compares favorably with the well-known TE materials.

In summary, we have discovered a family of high ZT TE materials, based on the quaternary chalcogenides of $\text{Cu}_2\text{ZnSnQ}_4$ ($Q=\text{S, Se}$), with an unusually large band gap ($>1.4 \text{ eV}$) yet with high p -type conductivity. Their distorted diamondlike structure endows them with low lattice thermal conductivities, whereas Cu doping on the Zn site increases hole conductivity and decreases thermal conductivity. Both the power factor and ZT increase with the temperature: at 700 K, $\text{Cu}_{2.1}\text{Zn}_{0.9}\text{SnSe}_4$ has a ZT of 0.45, which increases to 0.91 at 860 K. Therefore, these materials may be especially suitable for high temperature applications.

Financial support from National 973 Program of China (Grant Nos. 2007CB936704 and 2009CB939903), National Science Foundation of China (Grant No. 50772123), Science and Technology Commission of Shanghai (Grant No. 0752nm016), and Science and the Innovation Group of International Cooperation Plan (Grant No. 50821004) are acknowledged. I.W.C. acknowledges support of U.S. National Science Foundation (Grant Nos. DMR-07-05054 and DMR-05-20020).

¹P. Pecheur and G. Toussaint, *Phys. Lett. A* **135**, 223 (1989).

²P. Larson, S. D. Mahanti, and M. G. Kanatzidis, *Phys. Rev. B* **61**, 8162 (2000).

³G. S. Nolas, J. Sharp, and H. J. Goldsmid, *Thermoelectrics, Basic Principles and New Materials Developments* (Springer, New York, 2001), p. 121.

⁴J. O. Sofo and G. D. Mahan, *Phys. Rev. B* **58**, 15620 (1998).

⁵Y. Z. Pei, L. D. Chen, W. Zhang, X. Shi, S. Q. Bai, X. Y. Zhao, Z. G. Mei, and X. Y. Li, *Appl. Phys. Lett.* **89**, 221107 (2006).

⁶C. Keffer, T. M. Hayes, and A. Bienenstock, *Phys. Rev. Lett.* **21**, 1676 (1968).

⁷T. Su, X. Jia, H. Ma, J. Guo, Y. Jiang, N. Dong, L. Deng, X. Zhao, T. Zhu, and C. Wei, *J. Alloys Compd.* **468**, 410 (2009).

⁸See EPAPS Document No. E-APPLAB-94-002919 for supplementary tables and figures. For more information on EPAPS, see <http://www.aip.org/pubservs/epaps.html>.

⁹R. K. Bhandari, Y. Hashimoto, and K. Ito, *Jpn. J. Appl. Phys., Part 1* **43**, 6890 (2004).

¹⁰M. L. Liu, Y. M. Wang, F. Q. Huang, L. D. Chen, and W. D. Wang, *Scr. Mater.* **57**, 1133 (2007).

¹¹M. L. Liu, F. Q. Huang, L. D. Chen, Y. M. Wang, Y. H. Wang, G. F. Li, and Q. Zhang, *Appl. Phys. Lett.* **90**, 072109 (2007).

¹²M. L. Liu, F. Q. Huang, and L. D. Chen, *Scr. Mater.* **58**, 1002 (2008).

¹³S. Fiechter, M. Martinez, G. Schmidt, W. Henrion, and Y. Tamm, *J. Phys. Chem. Solids* **64**, 1859 (2003).

¹⁴J. Rivet, O. Gorochoy, and J. Flahaut, *C. R. Acad. Sci.* **260**, 178 (1965).

¹⁵L. I. Berger and N. A. Bulyonkov, *Izv. Akad. Nauk U.S.S.R. Phys.* **28**, 1100 (1964).

¹⁶G. Marcano, C. Rincón, L. M. Chalbaud, D. B. Bracho, and G. S. Pérez, *J. Appl. Phys.* **90**, 1847 (2001).

¹⁷I. V. Dudchak and L. V. Piskach, *J. Alloys Compd.* **351**, 145 (2003).

¹⁸R. Adhi Wibowo, E. S. Lee, B. Munir, and K. H. Kim, *Phys. Status Solidi A* **204**, 3373 (2007).

¹⁹G. S. Babu, Y. B. K. Kumar, P. U. Bhaskar, and V. S. Raja, *Semicond. Sci. Technol.* **23**, 085023 (2008).

²⁰H. Matsushita, T. Maeda, A. Katsui, and T. Takizawa, *J. Cryst. Growth* **208**, 416 (2000).

²¹S. R. Hall, J. T. Szymański, and J. M. Stewart, *Can. Mineral.* **16**, 131 (1978).

²²W. Schäfer and R. Nitsche, *Mater. Res. Bull.* **9**, 645 (1974).

²³M. L. Liu, L. B. Wu, F. Q. Huang, L. D. Chan, and J. A. Ibers, *J. Solid State Chem.* **180**, 62 (2007).